Complexity of the Mw6.3, 2009 L'Aquila (Central Italy) earthquake rupture

F. Gallovič, J. Zahradník, K. Vachek

Dept. of Geophysics, Faculty of Mathematics and Physics, Charles University in Prague, Czech Republic, gallovic@karel.troja.mff.cuni.cz; http://geo.mff.cuni.cz/~gallovic/

1. Abstract

The observed records (<0.2Hz) are analyzed by a newly proposed inversion technique. The source is parameterized by Multiple Finite-Extent (MuFEx) subsources, each with individual set of trial nucleation positions, rupture velocities and nucleation times. Grid-searching all combinations of the subsource parameters provides a database of plausible models. Besides providing a best-fitting model, the database allows also for the uncertainty analysis. The required preliminary setup is based on a technique free of constraints (e.g., on rupture velocity), namely the truncated singular value decomposition (TSVD) and the iterative multiple-point source deconvolution (ISOLA). The inversion confirms that the L'Aquila earthquake consisted of two major episodes, one in the up-dip direction immediately after the nucleation, while the other with along-strike propagation being delayed by 3-4s.

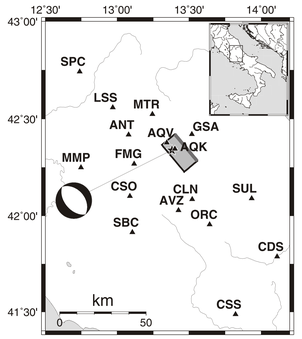

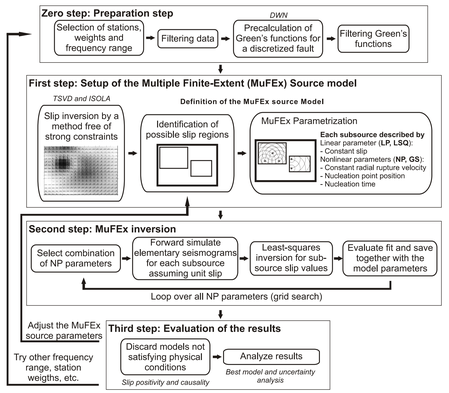

2. Synthetic test of the inversion

TSVD inversion [Gallovič and Zahradník, 2011]

- Based on a linear formulation utilizing discretized version of the representation theorem [Aki and Richards, 2002]
- Slip velocity time history without any constraints (only finite duration of 10s); the rupture propagation and shape of the slip velocity functions are not constrained and the slip can occur anywhere on the fault and anytime during the given source duration.
- The positivity constraint on slip velocities applied using the NNLS approach [Lawson and Hanson, 1974]. To regularize the solution, only the leading singular vectors are used, which leads to the so-called Truncated SVD solution
- We found [Gallovič and Zahradník, 2011] that the leading singular vectors (composing the final solution) are smooth functions of time and space, thus no additional smoothing is required.

Multiple Finite-Extent (MuFEx) inversion

[Gallovič and Zahradník, 2012]

- The source consists of several (three in the present case) homogeneous rectangular subsources with constant rupture velocities.
- The best-fitting model as well as the uncertainty analysis is then performed by grid-searching all combinations of the subsource parameters.
- For each combination of the subsource parameters, the slip values are obtained by the least squares approach.

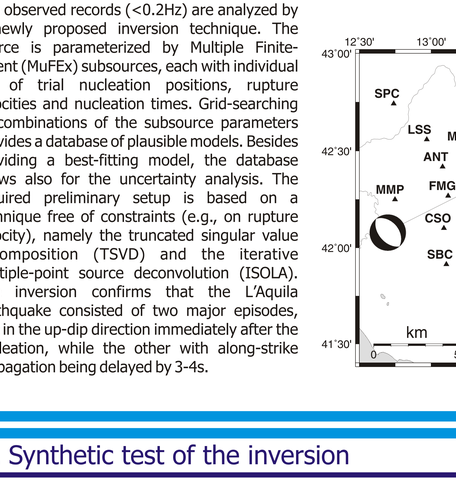

Fig. 1: A) Slip velocity snapshots of the input model with assumed constant rupture propagation from the hypocenter (star). B) Final slip of the input model. C) Snapshots of the model inverted by the TSVD approach with truncation at 1/10 of the largest singular value (to mimic a real-data application); variance reduction VR=0.98. The multiple point-source (ISOLA, Sokos and Zahradník, 2008) inversion is shown by green circles proportional to moment (the largest circle corresponding to 6.5x10^{17}Nm, VR=0.95). Here it is in a good agreement with TSVD. Areas with large slip velocities (or location of largest ISOLA point sources) are used for the first setup of the MuFEx subsources (shown as rectangles). D) Final slip of the inverted model. Comparing panels B and D, the inverted slip map is highly biased due to the effect of the truncation (regularization) during the TSVD inversion. The bottom right asperity is underestimated in TSVD; the top asperity is split into two by both TSVD and ISOLA.

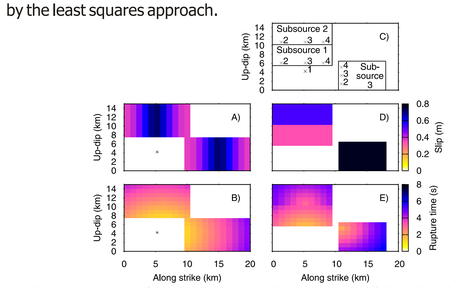

Fig. 2: Synthetic test of the inversion by the MuFEx source model. A) Final slip and B) rupture times of the input test model. Star denotes the hypocenter. C) Subsources of the MuFEx model. The numbered points represent trial nucleation points of the subsources. D) The best-fitting (grid-searched) MuFEx model in terms of final slip (assumed to be constant on the subsources) and E) rupture times (assuming a constant rupture velocity on each subsource). Panels D) and E) are to be compared with panels A) and B), respectively. Variance reduction VR=0.98.

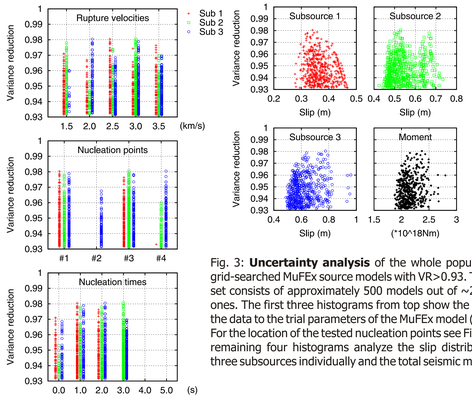

Fig. 3: **Uncertainty analysis** of the whole population of the grid-searched MuFEx source models with VR>0.93. The analyzed set consists of approximately 500 models out of ~2 million trial ones. The first three histograms from top show the sensitivity of the data to the trial parameters of the MuFEx model (see legend). For the location of the tested nucleation points see Figure 2C. The remaining four histograms analyze the slip distribution of the three subsources individually and the total seismic moment.

3. Inversion of real data

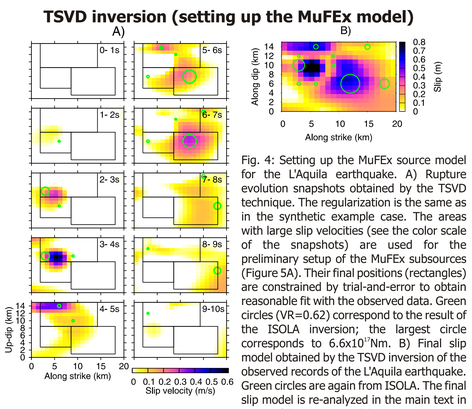

Fig. 4: Setting up the MuFEx source model for the L'Aquila earthquake. A) Rupture evolution snapshots obtained by the TSVD technique. The regularization is the same as in the synthetic example case. The areas with large slip velocities (see the color scale of the snapshots) are used for the preliminary setup of the MuFEx subsources (Figure 5A). Their final positions (rectangles) are constrained by trial-and-error to obtain reasonable fit with the observed data. Green circles (VR=0.62) correspond to the result of the ISOLA inversion; the largest circle corresponds to 6.6x10^{17}Nm. B) Final slip model obtained by the TSVD inversion of the observed records of the L'Aquila earthquake. Green circles are again from ISOLA. The final slip model is re-analyzed in the main text in terms of the MuFEx model.

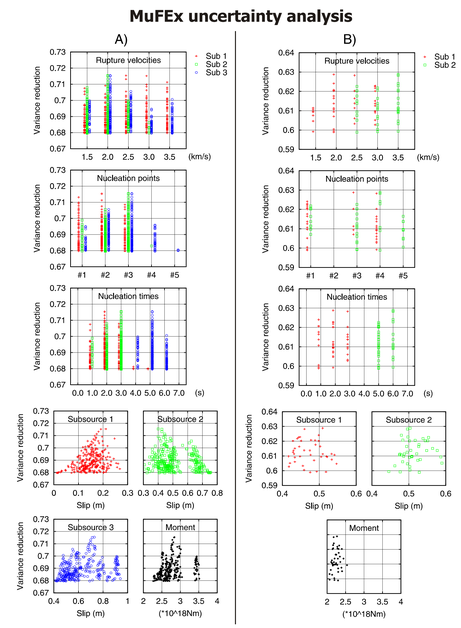

Fig. 7: **Uncertainty analysis** of the grid-searched MuFEx source models with VR>0.68 for the L'Aquila earthquake based on the (A) TSVD and (B) ISOLA preliminary inversions. The analyzed set consists of approximately 300 models out of 3 million trial ones. Let us emphasize that all the analyzed models are characterized by the delayed start of the subsource 3 (by 4-6s), observable also in the best fitting model in Figure 5.

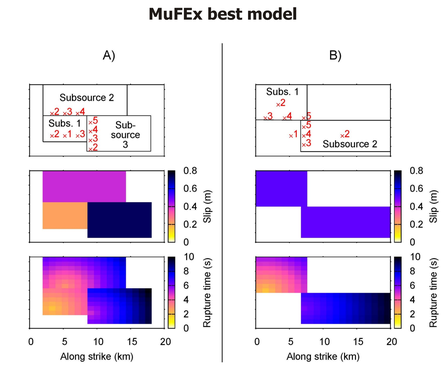

Fig. 5: Best fitting MuFEx model of the L'Aquila earthquake (VR=0.71, see Fig. 6). The trial nucleation points are shown in the top plot. The setup of the MuFEx subsources is based on the TSVD inversion (see Fig. 4). Note the time delay of the bottom right subsource.

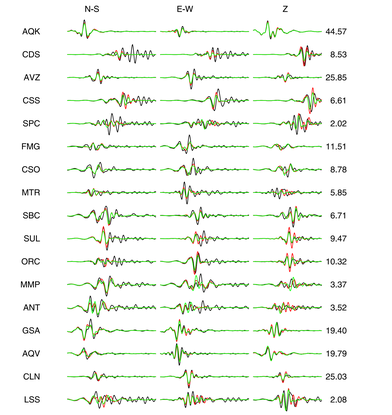

Fig. 6: Comparison between **observed (black)** and synthetic displacements for the L'Aquila event (red for the best-fitting MuFEx model of Figure 5A, green for the TSVD approach, VR=0.74). The records are band-pass filtered in the range 0.05-0.30Hz and have duration of 100s. Maximum amplitudes of the observed records in mm are shown as numbers.

3. Constraints from the GPS coseismic displacement data

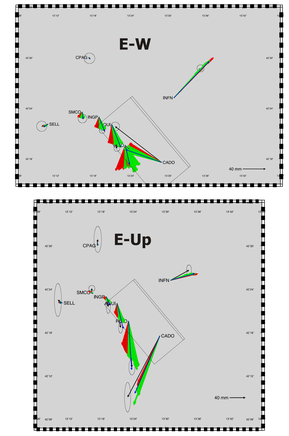

Fig. 8: GPS vectors for the MuFEx inversion (TSVD setup). **Black arrows**: observed data (Anzidei et al., 2009), red arrows: synthetics for all the MuFEx source models accepted in terms of the waveform fit, green arrows: MuFEx models best fitting the GPS vectors (VR>0.87).

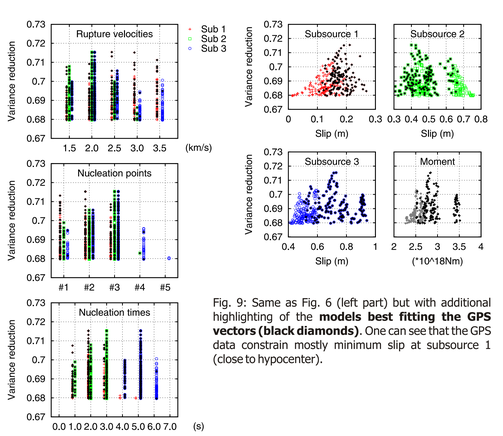

Fig. 9: Same as Fig. 6 (left part) but with additional highlighting of the **models best fitting the GPS vectors (black diamonds)**. One can see that the GPS data constrain mostly minimum slip at subsource 1 (close to hypocenter).

5. Conclusions

- In the present poster we investigate the near-fault recordings of the M6.3 2009 L'Aquila earthquake by means of the low-frequency slip inversion, with independent constraints from the GPS measurements.
- Uncostrained TSVD slip inversion provides biased results due to relatively strong regularization required. However, the method is a good indicator of major asperities, thus it is suitable for the subsequent Multiple-Finite Extent (MuFEx) source inversion.
- The MuFEx inversion provides not only the best-fitting source model but also it enables efficient uncertainty analysis of the inverted model. GPS data provide further constraint on plausible models.
- The remarkable robust feature of the L'Aquila earthquake are the rapid onset of the shallow asperity and the time delay of the second asperity. Unfortunately, we are unable to distinguish whether the latter was due to a temporal rupture arrest and a partial slow-down of the rupture.

References

Aki, K., and P. G. Richards (2002), Quantitative Seismology, Univ. Sci., Sausalito, Calif.

Anzidei, M., Boschi, E., Cannelli, V., Devoti, Esposito, A., Galvani, A., Melini, D., Pietrantonio, G., Riguzzi, F., Sepe, V., and E. Serpelloni (2009). Coseismic deformation of the destructive April 6, 2009 L'Aquila earthquake (central Italy) from GPS data, Geophys. Res. Lett. 36, L17307.

Bouchon, M. (1981), A simple method to calculate Green's functions for elastic layered media, Bull. Seism. Soc. Am. 71, 959-971.

Gallovič, F., and J. Zahradník (2011), Toward understanding slip-inversion uncertainty and artifacts II: singular value analysis, J. Geophys. Res., 116, B02309.

Gallovič, F., and J. Zahradník (2012), Complexity of the M6.3 2009 L'Aquila (central Italy) earthquake: 1. Multiple finite-extent source inversion, J. Geophys. Res. 117, B04307.

Lawson, C. L., and R. J. Hanson (1974), Solving Least Square Problems, Prentice-Hall, Inc., New Jersey, 340 pp.

Sokos, E., and J. Zahradník (2008), ISOLA A Fortran code and a Matlab GUI to perform multiple-point source inversion of seismic data, Computers & Geosciences, 34, 967-977.

Zahradník, J., and F. Gallovič (2010), Toward understanding slip-inversion uncertainty and artifacts, J. Geophys. Res., 115, B09310.

Acknowledgement: The authors acknowledge free Internet access of waveforms provided by the Italian Strong Motion Network (ITACA, http://itaca.mi.ingv.it/). Financial support: GACR 210/11/0854, MSM0021620860, Charles University project UNCE 204020/2012.